β-Cell mass restoration by α7 nicotinic acetylcholine receptor activation

Dhananjay Gupta, Adam A. Lacayo, Shane M. Greene, John L. Leahy, and Thomas L. Jetton[1]

From the Division of Endocrinology, Diabetes, and Metabolism, Department of Medicine, Larner College of Medicine, University of Vermont, Burlington, Vermont 05446

Edited by Jeffrey E. Pessin

Although it is well-established how nutrients, growth factors, and hormones impact functional β-cell mass (BCM), the influence of the central nervous system in this regard, and especially in the context of islet immune modulation, has been understudied. Here we investigated the expression and activity of pancreatic islet α7 nicotinic acetylcholine receptor (α7nAChR) in islet anti-inflammatory and prosurvival signaling. Systemic administration of α7nAChR agonists in mice improved glucose tolerance and curtailed streptozotocin-induced hyperglycemia by retaining BCM, in part through maintaining Pdx1 and MafA expression and reducing apoptosis. α7nAChR activation of mouse islets *ex vivo* led to reduced inflammatory drive through a JAK2–STAT3 pathway that couples with CREB/Irs2/Akt survival signaling. Because the vagus nerve conveys anti-inflammatory signals to immune cells of the spleen and other nonneural tissues in the viscera by activating α7nAChR agonists, our study suggests a novel role for β-cell α7nAChR that functions to maintain β-cell survival and mass homeostasis through modulating islet cytokine and phosphatidylinositol 3-kinase–dependent signaling pathways. Exploiting these pathways may have therapeutic potential for the treatment of autoimmune diabetes.

Normal immune system function in the viscera requires modulation by the central nervous system. Consequently, key pathological manifestations of type 1 diabetes (T1D)[2] include autonomic dysfunction, islet inflammation, and β-cell immune destruction (1–3). The autonomic nervous system (ANS) via the vagus nerve normally regulates a host of homeostatic processes including pancreatic islet function (4) as well as proinflammatory processes through the so-called "cholinergic anti-inflammatory system" (5–7). This system curtails innate immune system overactivity to maintain homeostasis in response to a range of inflammatory insults and disease states. The central cellular player for this system is the ligand-gated ion channel α7 nicotinic acetylcholine receptor (α7nAChR or "α7R"), widely expressed in the brain (8), autonomic ganglia (9), and reticuloendothelial system (10) but also in pancreatic β-cells (11, 12). This system requires α7R activation in cells of the reticuloendothelial system (classically splenic immune cells) via vagal stimulation with reduced NF-κB signaling activity leading to decreased proinflammatory cytokine expression (5–7). Although the role of the cholinergic branch of the ANS on β-cell function in human islets has been questioned in a study that found that α-cells impact β-cell function through paracrine secretion of ACh (13), a subsequent study suggests that autonomic signaling through nicotinic receptors B2 and B4 plays an important role in insulin secretion (14). Hence, distinct mechanisms of cholinergic input to β-cells appear to underlie the regulation of β-cell function *versus* growth and survival signals.

The hallmark of T1D is the immune-mediated destruction of insulin-producing β-cells (1, 2, 15). A complex interplay between islets and immune cells results in the local release of proinflammatory cytokines (IL-1β, TNFα, and IFNγ), triggering NF-κB–mediated up-regulation of iNOS (16). These cytokine effects are β-cell–specific. Chronically induced iNOS increases nitric oxide (NO) generation, which triggers islet dysfunction and, in the long-term, iNOS-dependent and -independent pathways of proinflammatory cytokine signaling, causing β-cell apoptosis (17–19). For T1D-susceptible individuals, it is critical to devise therapeutic strategies to counter the inflammatory drive to preserve islet function and survival during early inflammatory states.

As opposed to the β-cell muscarinic receptor 3 (M$_3$R) (20), and more recently, β-cell β2/β4nACh receptors (14) with defined roles in β-cell function, a role for β-cell α7R has not been fully elucidated. However, nicotine itself (a nonspecific nAChR agonist) has been shown to reduce T1D in rodent models, although its mechanism of action and the pancreatic cell types involved are unknown (21). Recently, central and systemic acetylcholinesterase inhibition has been found to prevent T1D (22) and T2D (23) in rodents. However, to date, there are no studies demonstrating whether *β-cell* α7R activation may contribute to the observed improvement of glucose homeostasis in mouse models of diabetes. The objective of this study was to determine the efficacy of specific α7R agonists to prevent, delay the onset of, or reduce the severity of multiple low-dose

[2] The abbreviations used are: T1D, type 1 diabetes; ANS, autonomic nervous system; BCM, β-cell mass; ACh, acetylcholine; α7nAChR or α7R, α7 nicotinic acetylcholine receptor; iNOS, inducible nitric-oxide synthase; M$_3$R, muscarinic receptor 3; STZ, streptozotocin; MLDS, multiple low-dose STZ; PNU, PNU-282987; KD, knockdown; MLA, methyllycaconitine; Het, haplo-deficient; CREB, cAMP-responsive element–binding protein.; Veh, vehicle; i.p., intraperitoneal; IPGTT, intraperitoneal glucose tolerance test; TUNEL, deoxynucleotidyltransferase-mediated dUTP nick end labeling.
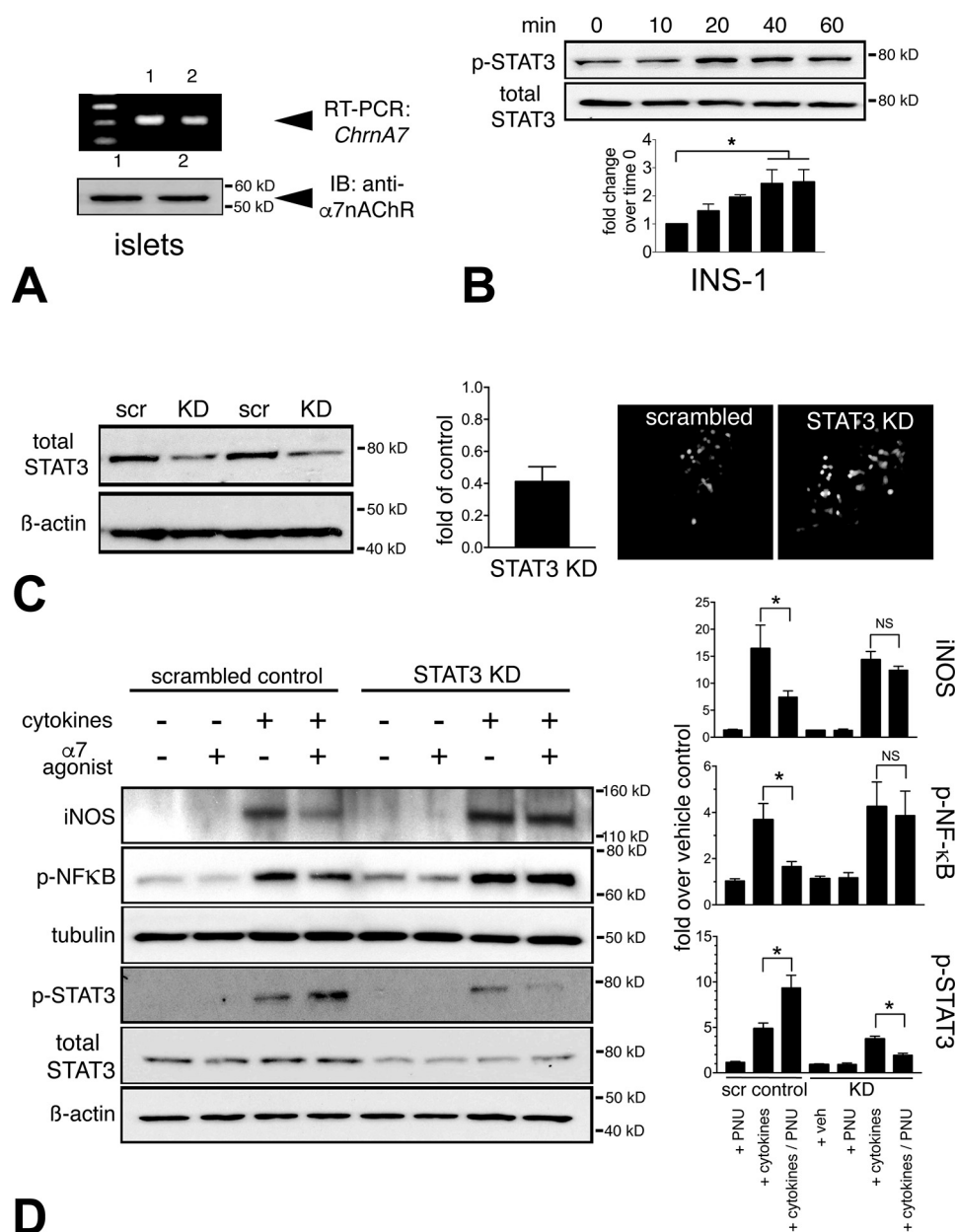
Figure 1. STAT3 dependence of α7nAChR anti-inflammatory signaling in β-cells. *A*, β-cells express α7R. RT-PCR reveals *Chrna7* expression (encoding α7R) in mouse islets (*upper panel*) corroborates anti-α7R immunoblot (*IB*, *lower panel*). *B*, time course of α7R-mediated STAT3 phosphorylation (Thr[705]) in INS-1 cells. INS-1 cells were treated with α7R agonist (PNU, 100 μM) in heat-inactivated serum medium. Cell lysates were collected at intervals of 10 min, and immunoblotting was performed for phosphorylated and total STAT3. Band densitometry demonstrates that α7R agonist led to progressive STAT3 phosphorylation, peaking at 60 min (*, $p < 0.05$). *C*, generation of INS-1 cells with shRNA-mediated stable KD of STAT3 protein and scrambled shRNA control (*scr*). INS-1 cells were transfected with either GFP-tagged shRNA or scrambled shRNA as a control, and GFP-positive INS-1 cells were obtained through puromycin selection. Effective STAT3 KD was determined by immunoblot assessing total STAT3 protein levels. STAT3 protein level in the selected KD clone was reduced 60% compared with the scrambled control. These are representative live cell fluorescence images of GFP-positive shRNA and scrambled control INS-1 cells. *D*, INS-1 cells exhibit STAT3-dependent activation of α7R, required for anti-inflammatory signaling. Representative immunoblots from INS-1 cells with STAT3 KD and control cells subjected to proinflammatory cytokine challenge (TNFα, IL-1β, and IFNγ) ± PNU treatment reveal reduced proinflammatory signaling through decreased phospho-NF-κB and increased phospho-STAT3 levels, resulting in reduced iNOS induction in scrambled control shRNA INS-1 cells, which was abrogated in INS-1 cells with STAT3 KD. Band intensity quantitation was performed from three separate blots (*, $p < 0.05$).

STZ (MLDS) diabetes, which models certain features of T1D, and to resolve the role of β-cell α7R in this improvement.

Results

β-Cells express α7nAChR and exhibit STAT3 activation–dependent anti-inflammatory signaling

We verified that α7R is expressed in pancreatic β-cells in rodents (11, 12). By quantitative real-time PCR, we detected

Chrna7 (α7nAChR) mRNA in INS-1 insulinoma cells (not shown) as well as in normal mouse islets (Fig. 1*A*, *top*). This was corroborated at the protein level by immunoblot (Fig. 1*A*, *bottom*). Prior studies in immune cells have demonstrated that α7R is a critical effector of anti-inflammatory signaling through the JAK2–STAT3 signaling pathway (24, 25). We tested α7R-mediated activation of STAT3 by treating INS-1 cells with PNU-282987 (PNU) (100 μM), a complete and highly specific

α7R agonist, and observed a time-dependent phosphorylation of tyrosine (Thr[705]) of STAT3, reaching a peak at 60 min with a 2.4-fold increase compared with vehicle-treated INS-1 cells (Fig. 1*B*). To test STAT3 dependence on α7R activation, we created a constitutive knockdown (KD) of STAT3 in INS-1 cells by transfecting GFP-tagged shRNA against STAT3 and used GFP-tagged scrambled shRNA as a control (Fig. 1*C*). We achieved an effective 60% reduction of STAT3 protein levels in a GFP-positive shRNA clone compared with a scrambled shRNA STAT3 control INS-1 cells (Fig. 1*C*). The STAT3 KD and scrambled control transfected INS-1 cells were next challenged with a mixture of proinflammatory cytokines (TNFα, IL-1β, and IFNγ) to test STAT3 dependence on α7R signaling. Accordingly, cytokine stimulation of scrambled control STAT3 INS-1 cells resulted in a 3.6-fold increased phosphorylation and activation of NF-κB over the vehicle control, concomitant with a 16-fold induction of iNOS protein levels (Fig. 1*D*). Pretreatment and continued exposure of INS-1 cells with the α7R agonist during the cytokine challenge in the scrambled control STAT3 cells reduced the extent of NF-κB phosphorylation (to 1.65-fold increased) as well as lowering the induction of iNOS protein levels (to 7.4-fold increased) (Fig. 1*D*). Whereas the cytokine mixture alone activated STAT3 (4.8-fold increased), the α7R agonist further increased STAT3 phosphorylation (9-fold), resulting in reduced iNOS induction, likely through an interaction with NF-κB as demonstrated previously (25, 26). The inhibitory effects of α7R activation on NF-κB phosphorylation and iNOS protein induction was completely lost under proinflammatory cytokine challenge in the STAT3 KD INS-1 cells, resulting in reduced phosphorylated and total STAT3 protein (Fig. 1*D*). Collectively, proinflammatory cytokine challenge experiments in the INS-1 cells with STAT3 KD demonstrated that STAT3 signaling is an integral component of anti-inflammatory action mediated by the α7R pathway.

We next performed isolated B6N mouse islet experiments to evaluate α7R agonist–mediated activation of STAT3 signaling. A 1-h treatment of isolated mouse islets with α7R agonist PNU (100 μM) caused a 2-fold increase in the phosphorylation of tyrosine (Thr[705]) on STAT3 protein (Fig. 2*A*), similar to INS-1 cells (Fig. 1*B*). We further tested the anti-inflammatory effects of α7R agonist–mediated activation of STAT3 signaling in islets subjected to a proinflammatory cytokine challenge by pretreatment (1 h) with the PNU agonist or a specific antagonist, methyllycaconitine (MLA) (100 nM), comparing it to vehicle (DMSO)-treated controls. These treatments either increased or decreased STAT3 phosphorylation, respectively, leading to reduced or enhanced NF-κB proinflammatory signaling (Fig. 2*B*). Whereas iNOS was induced 12.5-fold over the control in cytokine-treated islets alone, upon PNU pretreatment, the iNOS induction signal was reduced to 4.7-fold over the control. MLA pretreatment of islets essentially maintained cytokine-induced iNOS generation. Phosphorylated NF-κB, correlated with its increased proinflammatory activity, was reduced in PNU-treated islets (1.4- *versus* 3.1-fold in cytokine only) (Fig. 2*B*). Because phospho(Thr[705])-STAT3 correlates with reduced proinflammatory drive (25), in the cytokine alone–treated islets, the phospho-STAT3 signal was reduced to 28% of the control islets (no cytokine). However, PNU treat-

ment restored phospho-STAT3 levels to 114% of the control levels, and MLA treatment maintained reduced phospho-STAT3 levels (21% of control) (Fig. 2*B*). Thus, β-cell anti-inflammatory signaling via JAK2/STAT3 can be activated by direct α7R stimulation. Hence, systemically delivered α7 agonists likely target pancreatic β-cells directly, in addition to other tissues, to execute their anti-inflammatory action.

Islet anti-inflammatory signaling depends on Chrna7 expression

To assess the specificity of PNU action through α7R, we tested the anti-inflammatory effects of α7R signaling in isolated mouse islets subjected to a proinflammatory cytokine challenge in islets from *Chrna7* haplodeficient (Het) and *Chrna7* KO mice. Whereas Het mouse islets retain a PNU-stimulated reduction in iNOS generation similar to WT islets, as demonstrated in Fig. 2*C*, islets from *Chrna7* KO mice treated with PNU exhibit no reduction in iNOS levels. Therefore, curtailment of cytokine-induced iNOS generation with PNU depends on at least one functional *Chrna7* gene copy.

β-Cells exhibit α7nAChR-dependent Akt/Irs2 growth and survival signaling

The α7R is the central effector of the vagus nerve–mediated anti-inflammatory reflex. We established previously that a bilateral celiac branch vagotomy in normal Sprague-Dawley rats leads to a transient loss of activated β-cell Akt and signaling that correlated with reduced proliferation (27). This suggested that the celiac branches of the vagus nerve convey β-cell growth and survival signals. Although the nature of this effect was unresolved, we surmised that the highly expressed M$_3$R acetylcholine receptor was unlikely to play a role because β-cell specific manipulation of M$_3$R levels in mice failed to show a BCM/growth phenotype (20). Accordingly, to explore potential cross-talk through β-cell α7R signaling with downstream canonical growth and survival pathways, we examined Irs2/Akt signaling in WT and *Chrna7* KO mouse islets stimulated *ex vivo* with PNU for 72 h. In the WT mouse islets, PNU treatment elicited a marked increase in Irs2 and phospho-Akt levels that was not observed in islets from *Chrna7* null mice (Fig. 3). Furthermore, α7R-dependent increases in activated (phospho-Ser[133]) CREB and Pdx1 were also observed in mouse islets upon PNU stimulation (Fig. 3). These responses were lost in *Chrna7* null mice. Collectively, these data suggest that β-cell anti-inflammatory drive and growth/survival signaling pathways may be activated by direct α7R stimulation and provide mechanistic insight into the roles of β-cell α7R in the observed functional BCM retention in the STZ diabetic mice.

α7nAChR agonists improve glucose homeostasis in MLDS mice

We next examined the effects of α7R agonists in MLDS mice. To examine the effects of α7R agonist treatment on β-cell pathophysiology in the context of autoimmune-mediated β-cell destruction, we treated B6N mice with an α7R agonist (10 mg/kg, i.p.) or a vehicle solution (Veh) (DMSO/PBS) and induced diabetes with a standard MLDS regimen. This model mimics several features of T1D with islet inflammation and
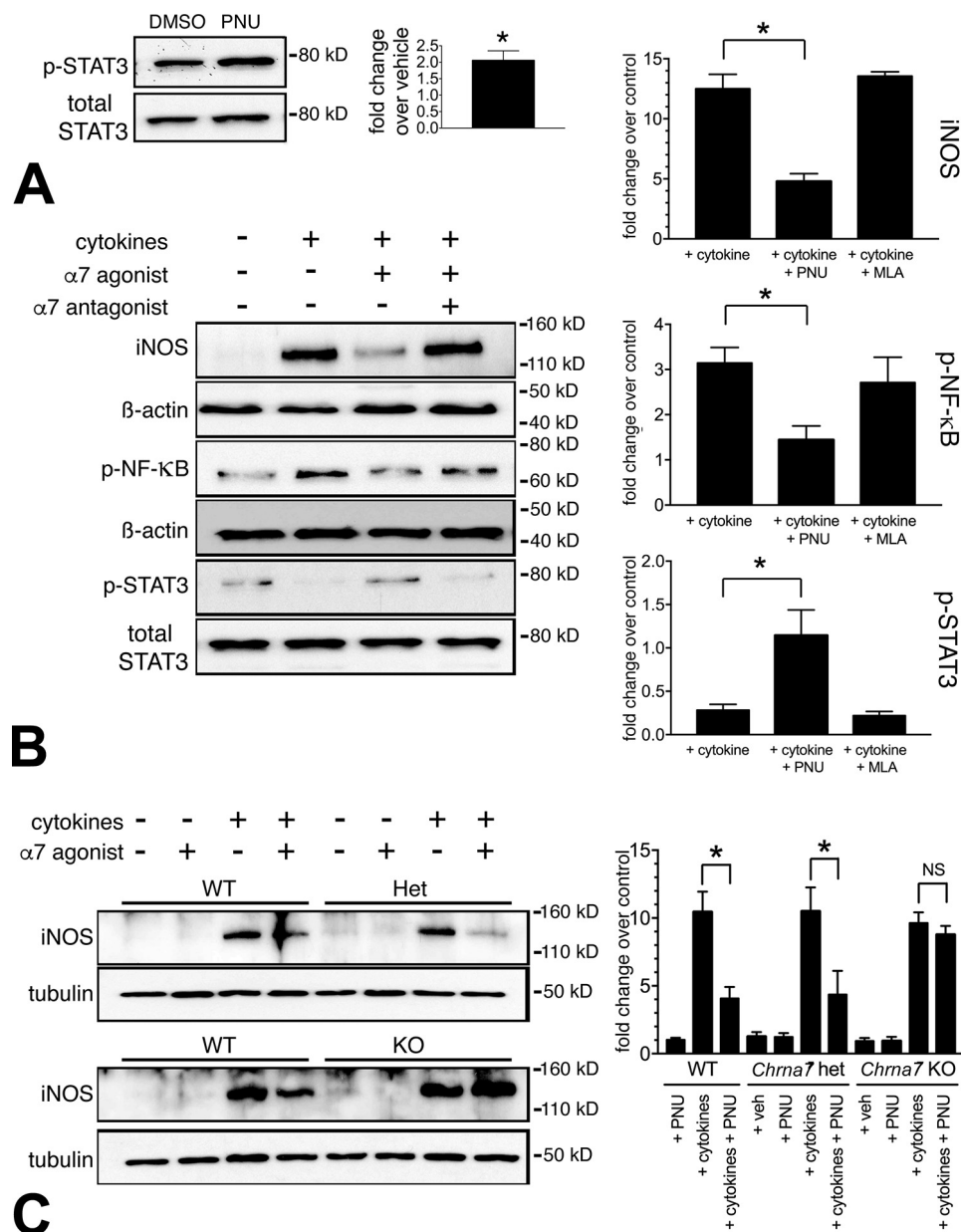
Figure 2. Cultured islets display α7nAChR-specific anti-inflammatory signaling. *A*, α7R agonist (PNU) treatment increased p-STAT3 (Thr^{705}) levels 2-fold compared with vehicle-treated islets. Freshly isolated B6N islets were equilibrated overnight in a standard islet culture medium followed by a 1-h incubation in heat-inactivated serum–supplemented medium prior to exposure to α7R agonist (100 μM PNU for 1 h) or vehicle (DMSO). The densitometry data represent ratios of p-STAT3/total STAT3 performed on three separate experiments (*, $p < 0.05$). *B*, PNU curtailed proinflammatory marker expression in mouse primary islets, whereas its antagonist (MLA) restored proinflammatory marker expression in response to proinflammatory cytokine challenge. Freshly isolated islets were rested overnight in islet culture medium followed by a 1-h incubation in heat-inactivated serum–supplemented medium prior to exposure to α7R agonist or antagonist pretreatment before cytokine challenge. Shown are representative immunoblots and corresponding quantitation of inflammatory markers of islets subjected to cytokines and treated with α7R agonist or antagonist. Islet α7R activation drives the anti-inflammatory response with reduced phospho-NF-κB and increased phospho-STAT3 levels resulting in decreased iNOS induction, whereas α7R antagonism reverses the proinflammatory signaling response by inhibiting STAT3 phosphorylation and restoring phospho-NF-κB levels leading to enhanced iNOS levels. *C*, islet anti-inflammatory signaling depends on *Chrna7* expression. WT, *Chrna7* haplodeficient (Het), and *Chrna7* null (KO) islets underwent cytokine challenge as described under "Experimental procedures." Representative iNOS immunoblots and corresponding quantitation reveal that α7R agonist reduction of cytokine-induced iNOS generation depends on at least one functional *Chrna7* gene copy. Band intensity quantitation in *panels* was performed from three separate immunoblots (*, $p < 0.05$).

local cytokine release (28). From the array of commercially available α7R agonists, GTS-21, a partial agonist, was initially chosen for *in vivo* testing because it has an established safety profile in humans (29). However, as an intraperitoneal glucose tolerance test (IPGTT) in GTS-21–treated mice at 4 days following the last STZ injection revealed only a modest improvement in glucose tolerance (data not shown), we next tested the effects of the complete α7R agonist, PNU, in separate timed

cohorts of mice. At week 1 following the last STZ injection, a daily PNU treatment (10 mg/kg) resulted in a progressive reduction in both fasting (not shown) and fed glycemia through week 4 (Fig. 4*A*). STZ treatment caused a modest weight loss in the mice after 4 weeks, which was not affected by PNU treatment (not shown). IPGTT revealed a striking, progressive improvement in glucose homeostasis in PNU/STZ-treated mice (Fig. 4, *B* and *C*). We measured glucose-induced insulin
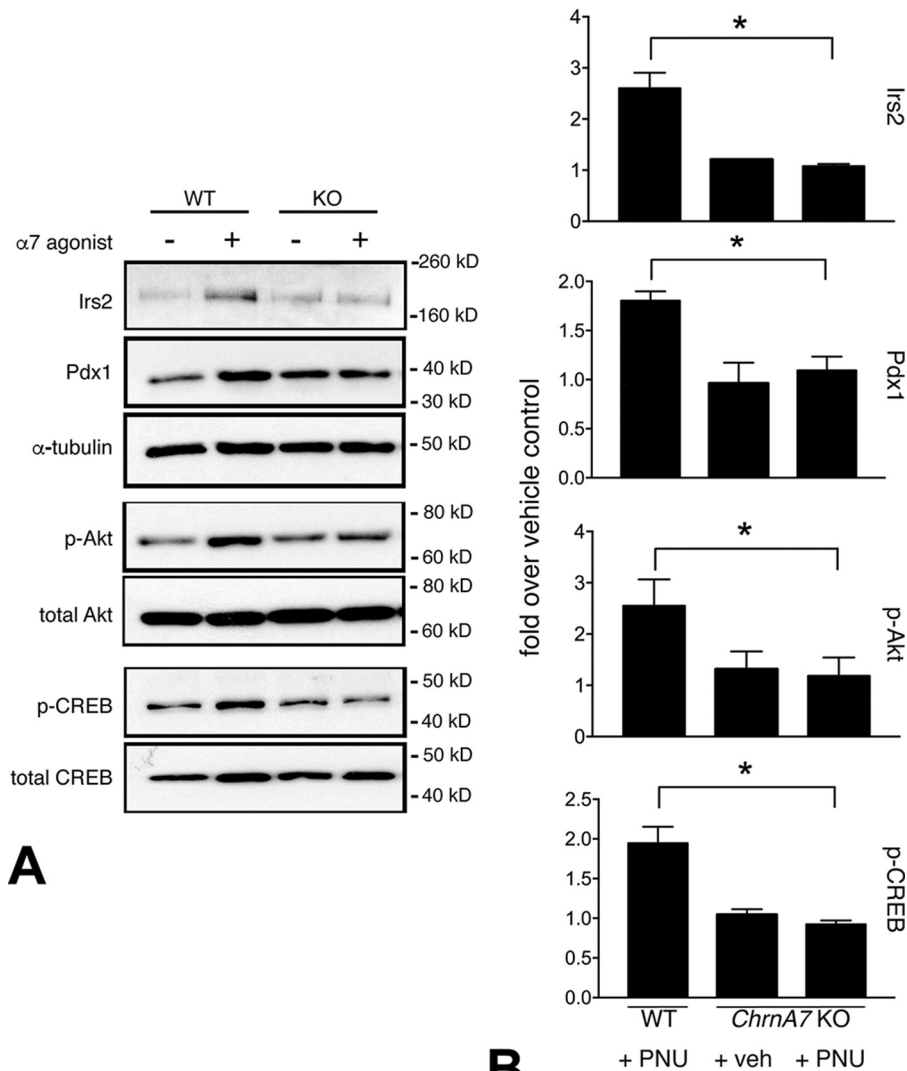
Figure 3. α7nAChR signaling displays cross-talk with growth and survival pathways. *A*, representative immunoblots of WT and *Chrna7* KO mice islets subjected to 72-h treatment (PNU) or vehicle control (DMSO) demonstrate enhanced expression of profunction and prosurvival markers. PNU stimulation leads to increased Irs2/Akt activation and augmented levels of the key β-cell transcription factor Pdx1 and the prosurvival factor CREB. Direct PNU stimulation of these factors in islets depended on α7R expression as evidenced by loss of these responses in islets from *Chrna7* null KO mice (*right panels*). *B*, band intensity quantitation for β-cell markers was performed from three separate immunoblots (*, $p < 0.05$). Comparisons were made using vehicle-treated WT islets as a reference.

secretion during the glucose tolerance test in the 2-week treatment cohort. Insulin secretion increased modestly in the PNU/STZ group but only at the 15-min time point (>1.6-fold improvement over the Veh/STZ group ($p < 0.05$, *t* test). Thus, a systemically delivered complete α7R agonist improves glucose homeostasis and partially restores β-cell function following MLDS diabetes induction.

α7nAChR agonism improves BCM in MLDS mice

We next sought to determine the basis of the glycemic improvement in PNU/STZ-treated mice after 4 weeks treatment using pancreas morphometry to measure potential changes in BCM and its contributing parameters. As anticipated, BCM was reduced (50%) in the vehicle-treated STZ control group (Veh/STZ) compared with the vehicle-treated control group ($p < 0.01$; Fig. 5A, Veh/Veh). Importantly, a 60% higher BCM was observed in the PNU/STZ-treated mice over that of the Veh/STZ mice ($p < 0.05$; Fig. 5A). To explore the

underlying mechanisms contributing to BCM retention, we measured β-cell proliferation, hypertrophy (β-cell size), apoptosis, and islet size distribution. Whereas β-cell proliferation was ~40% higher in the PNU/STZ group compared with both the PNU/Veh ($p < 0.01$) and Veh/Veh ($p < 0.05$) groups, proliferation was not significantly different between the PNU/STZ and the Veh/STZ groups (Fig. 5B). Therefore, β-cell proliferation appears unlikely to contribute to the greater BCM in the PNU/STZ group. Furthermore, individual β-cell size was not different among any of the groups (Fig. 5C). We conducted TUNEL staining in pancreatic sections from from week 2 and week 4 mice to mark apoptotic β-cells. Whereas the Veh/Veh and PNU/Veh groups exhibited no TUNEL$^+$ β-cells at either the 2- or 4-week time point, the 4-week Veh/STZ and PNU/STZ groups displayed very low numbers, which precluded a meaningful comparison. However, at the 2-week time point, the PNU/STZ group exhibited 60% reduced frequency in TUNEL$^+$
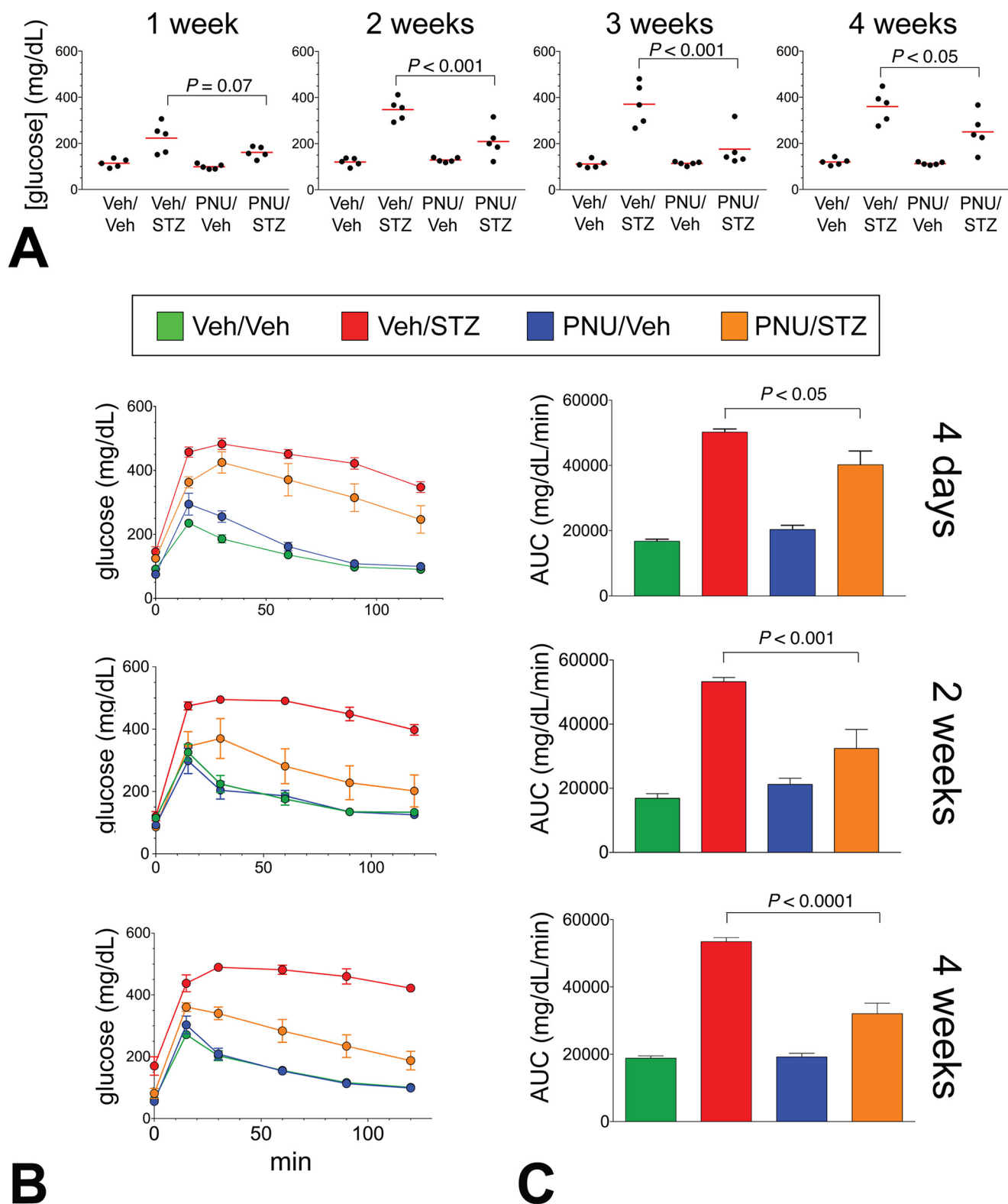
Figure 4. α7nAChR agonist treatment ameliorates STZ-induced diabetes in mice. *A*, weekly fed-blood glucose levels of STZ-induced or control mice subjected to daily injections of 10 mg/kg PNU-282987 or vehicle (4-week cohort). The mean values are indicated by *red bars*. *B*, PNU treatment improves glucose tolerance in MLDS mice as shown by IPGTT *curves*; and *C*, the corresponding area under curve (*AUC*) plots. All *p* values (using one-way analysis of variance) are indicated. The 4-day and 2-week cohorts were distinct from the mice used for the 4-week group. All groups, *n* = 5.

β-cells compared with the Veh/STZ group (Fig. 5D). We next compared the relative numbers of islets in specific size classes among the STZ-treated groups to provide insight into potential new islet growth (neogenesis or regeneration) and islet turn-over. We found greater numbers of smaller to medium-size islets in the PNU/STZ-treated mice compared with the Veh/STZ control group (Fig. 5E); however, there were no differences between the mouse treatment groups in the largest islet size
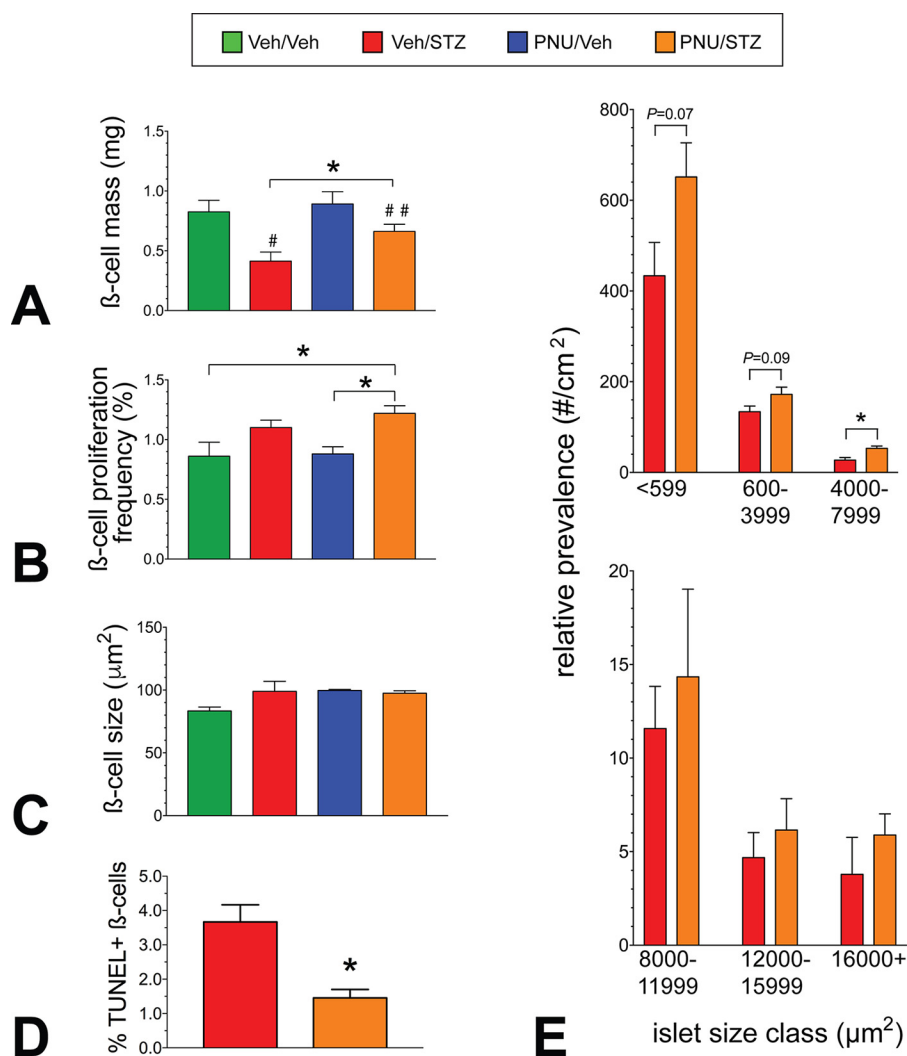
Figure 5. The glycemic improvement in PNU-282987–treated mice is a result of preserved β-cell mass. *A*, morphometric analysis reveals that although BCM is reduced 50% in the STZ control mice (#) compared with its respective control group after 4 weeks, the PNU-treated STZ mice showed no significant reduction in BCM (##) compared with the Veh/Veh and PNU/Veh groups. However, a 60% higher BCM (*, $p < 0.05$, *t* test) was observed in the PNU/STZ mice compared with the STZ control group. *B*, β-cell proliferation, as determined by Ki-67^{+}/insulin[+] cell staining, was greater in the PNU/STZ group as compared with the Veh/Veh and PNU/Veh groups (*, $p < 0.05$, *t* test) but not when compared with the STZ control group. *C*, There were no detectable differences in individual β-cell size among the groups. *D*, TUNEL[+] β-cell staining and quantitation in pancreatic sections from week 2 mice. Whereas the Veh/Veh and PNU/Veh groups exhibited no TUNEL[+] β-cells at either the 2- or 4-week time point, the PNU/STZ group exhibited 60% reduced β-cell apoptosis compared with the Veh/STZ group at the 2-week time point (*, $p < 0.01$, *t* test). *E*, β-cell cluster/islet size analysis comparison between the PNU/STZ *versus* Veh/STZ control group revealed a trend toward higher numbers in the smallest islet size classes but 2-fold higher (*, $p < 0.01$, *t* test) in the 4000–7999-μm^2 class (~65–90-μm diameter) (*upper panel*). No differences were observed in the larger islet size classes (*lower panel*). All groups, $n = 5$.

classes. Thus, the augmented BCM in the STZ/PNU-treated mice largely results from β-cell restoration/enhanced survival, but also there may be some contribution by islet regeneration and/or increased β-cell survival potential of small and intermediate islet size classes.

α7nAChR activation in MLDS mice leads to increased expression of key β-cell transcription factors

We reasoned that 4 weeks of daily α7R activation with PNU in MLDS mice resulting in improved glucose homeostasis and BCM retention would likely be regulated by β-cell factors that control growth, functional maturation, and survival. Accordingly, utilizing a high-resolution semiquantitative immunofluorescence analysis (27, 30) to measure the relative levels of key nuclear factors in individual β-cells and counting ~200 β-cells/mouse (range, 120–248 β-cells), we detected an ~70% increases in the nuclear signal of both Pdx1 and MafA in the PNU/STZ-treated group compared with the Veh/STZ group (Fig. 6*A*). Similar analysis for comparing nuclear-sited, activated (phospho-Ser[133]) CREB, a β-cell survival factor, revealed that nuclear p-CREB levels in the PNU-STZ mice were maintained at levels similar to that of the Veh/Veh control mice, but because of a marked variation in nuclear p-CREB immunoreactivity among different β-cells in an individual, no significant difference was observed between the PNU/STZ and Veh/STZ groups (Fig. 6*A*, *top panel*). Whereas mice from the Veh/Veh and PNU/Veh control groups exhibited β-cells with high levels of nuclear Pdx1 and MafA, β-cells from the Veh/STZ group displayed markedly reduced nuclear Pdx1 and MafA, as well as depleted insulin stores (Fig. 6*B*). These key transcription factors, and insulin to a lesser extent, were essentially restored in the PNU-treated STZ mice. Thus, it appears
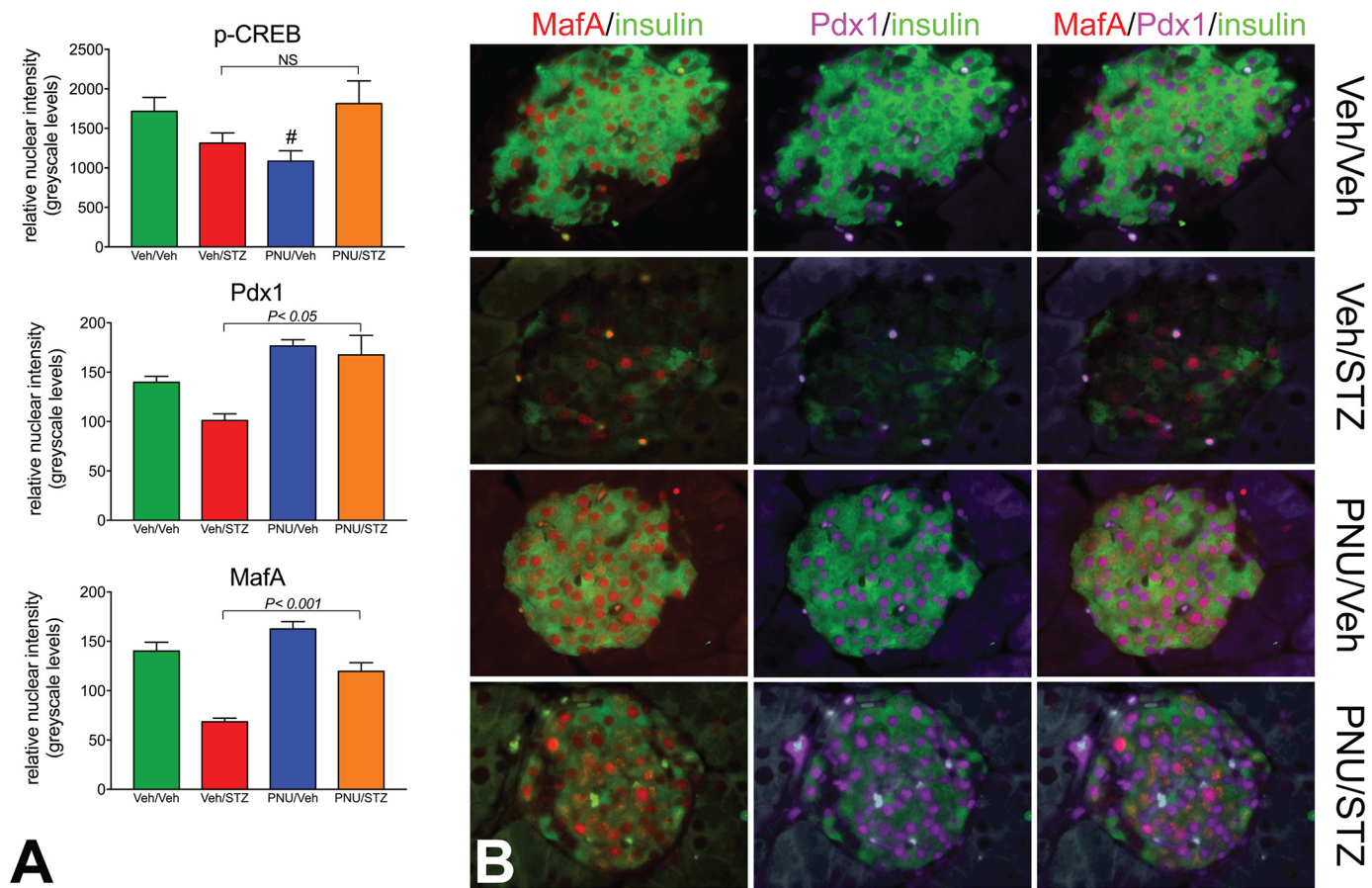
Figure 6. Glycemic improvement and β-cell mass retention from α7nAChR activation correlates with increased expression of key nuclear factors. *A*, normalization of activated CREB through α7R activation in STZ-induced mice (*top panel*). After 4 weeks of treatment, semiquantitative immunofluorescence analyses showed normalization of the β-cell nuclear phospho-Ser[133] CREB signal in β-cells of the PNU/STZ-treated group comparable with that of the Veh/Veh group, but no significant difference was seen between the PNU/STZ and Veh/STZ groups ($p = 0.13$) after 4 weeks. Nuclear phospho-CREB immunoreactivity was significantly reduced in the PNU/Veh mice (#, $p < 0.05$) compared with the Veh/Veh and PNU/STZ groups. Image analyses revealed ~70% increases in the β-cell nuclear signal of both Pdx1 and MafA in the PNU/STZ-treated group (*middle* and *bottom panels*) compared with the Veh/STZ group (*t* test, PNU/STZ *versus* Veh/STZ) after 4 weeks. *B*, representative fields of an islet from each animal group showing markedly reduced nuclear Pdx1 (*purple*) and MafA (*red*), as well as insulin, in the Veh/STZ group but restored nuclear Pdx1 and MafA in the PNU/STZ mice. Insulin immunostaining (*green*) marks β-cells.

that key transcription factors controlling β-cell functional maturation (Pdx1 and MafA) and survival (Pdx1 and to a lesser extent CREB) are up-regulated following MLDS induction preceded by α7R agonist treatment.

Discussion

Autonomic dysfunction and inflammation are key features of T1D. Normal homeostatic maintenance requires central nervous system regulation of digestion and nutrient metabolism as well as control of inflammation. Data are mounting on the primacy of autonomic failure (5, 6, 31), including early islet nerve loss (32, 33), in the progression of inflammatory cascades leading to autoimmune diabetes. Furthermore, pancreatic islet cholinergic drive may be reduced, in part because of enhanced β-cell acetylcholinesterase activity in early stages of the disease (34), implicating altered ACh levels in pathological changes leading to β-cell apoptosis. Islet ACh signaling through two distinct receptor types, muscarinic and nicotinic, has been studied with respect to β-cell function, growth, and survival. Because the β-cell–specific KO of *Chrm3* (encoding M₃R) in mice shows no BCM phenotype (20), this functionally important and highly expressed muscarinic AChR is unlikely to play a

role in β-cell survival. However, preclinical studies have established that nicotine administration (21) or nonspecific pharmacologic cholinergic stimulation can reverse the development or prevent T1D (22, 35) and T2D (23). Our aim in the current study was to test whether specific agonists activating the α7R, a ligand-gated ion channel with a well-defined role in the cholinergic anti-inflammatory pathway, might provide protection from mouse T1D development and to examine how the β-cell α7R might contribute to this improvement.

We demonstrated in a MLDS mouse model that a 3-day pretreatment with a systemic α7R agonist (PNU-282987) followed by a daily treatment reduced hyperglycemia, improved glucose homeostasis, and preserved BCM. BCM is the product of β-cell turnover, dictated by new cell recruitment by proliferation or neogenesis, and cell death via apoptosis and clearance. Whereas we found that proliferation played no role in BCM augmentation in the PNU/STZ group compared with the control/STZ group, there was a minor contribution of neogenesis and/or the preferential retention of the smaller to medium-size islets by 4 weeks of treatment. However, it appears that the major means of BCM restoration, as determined by TUNEL

staining at the 2-week time point, is reduced β-cell apoptosis. Collectively, the morphometric data suggest that α7R agonist treatment promotes BCM preservation by enhancing β-cell survival. This contention is based on the normal physiological adaptive mechanisms that drive homeostasis. Accordingly, the vagus nerve, in addition to its well-established roles in regulating digestion and islet secretory function for glucose homeostasis, has a role in maintaining organ mass and regeneration. For instance, the ANS via the hepatic vagus nerve controls liver regeneration by modulating both proliferation and apoptosis (reviewed in Ref. 36). Similarly, the vagus nerve also mediates signals that control β-cell proliferation (27, 37–39), and vagal interruption to the pancreas in normal rats leads to a transient loss of β-cell proliferation as well as reduced growth and survival signals (27). Thus, α7R activation in the context of MLDS mice may partially mimic the efferent components of normal vagal activity.

Because in the current study α7R activation in T1D-prone mice promoted BCM retention without significantly impacting β-cell proliferation, we concluded that α7R signaling at the level of the β-cell may primarily drive prosurvival/anti-inflammatory activity. This was supported by our *in vitro* data in INS-1 cells and mouse islets demonstrating α7R-mediated prosurvival signaling (via CREB and Akt/Irs2) concomitant with reduced inflammatory drive (via STAT3-dependent NF-κB modulation of iNOS expression). Furthermore, PNU-282987 anti-inflammatory activity was lost in islets from *Chrna7* null mice, confirming the specificity of the agonist. Our data in MLDS mice also support enhanced β-cell survival signaling upon α7R activation as evidenced by increased nuclear Pdx1 levels and a trend toward enhanced activated (phospho-)CREB levels that reduce apoptosis. Pdx1 has been ascribed a prosurvival function (40) in addition to its pivotal role in transactivating key β-cell genes such as *MafA*, which we found increased concordantly with Pdx1 following α7R activation. These data support the hypothesis that α7R agonist treatment, in the context of MLDS-induced islet inflammation, preserves BCM by reducing proinflammatory drive and enhancing survival. Our results are also in accord with a recent study demonstrating that nonspecific nAChR activation attenuates inflammatory cytokine-mediated β-cell apoptosis in mouse and human islets by reducing endoplasmic reticulum stress and alleviating the mitochondrial/Bcl2 protein-driven apoptotic cascade (41).

Manipulation of α7R activity with nicotine and PNU-282987 has been shown to enhance insulin sensitivity in normal rats and nonobese insulin-resistant mice in a STAT3-dependent fashion (42). Interestingly, this pathway, active in skeletal muscle, adipose, and liver, seems to be independent of the anti-inflammatory cascade (42). As no obvious enhancement of glucose tolerance was observed in PNU/Veh-treated mice compared with the Veh/Veh control B6N WT mice, potential α7R agonist effects on insulin sensitivity in non-STZ mice seems unlikely. On the other hand, because PNU treatment only modestly restored glucose-induced insulin secretion, an α7R-mediated effect on enhancing insulin sensitivity in the PNU/STZ mice is likely. Future studies are warranted to test whether PNU treatment may improve insulin sensitivity in the MLDS model.

A well-established role for the vagus nerve is to balance and dampen the proinflammatory drive. In animal studies, the efferent arm of this regulatory loop, the cholinergic anti-inflammatory pathway, can be mimicked by systemic pharmacologic manipulation to reduce islet inflammatory cytokine expression. Of particular importance, Mabley *et al.* (21) have established that nicotine, a general nAChR agonist, reduces T1D incidence in both MLDS and NOD mouse models by stimulating the switch of pancreatic Th1 to Th2 cytokine levels, decreasing proinflammatory cytokine expression while enhancing IL-4 and IL-10 expression, and reducing NO production. The current study establishes that a brief 3-day pretreatment with a specific α7R agonist followed by daily treatments superimposed with a standard 5-day MLDS induction resulted in glycemic improvement and BCM restoration in concert with enhanced β-cell survival signaling. Our data correlate well with a recent study by George *et al.* (22) wherein mice pretreated for 3 weeks with a specific and potent acetylcholinesterase inhibitor (paraoxon), systemically increasing ACh levels, were subjected to a similar MLDS regimen. In this context, both muscarinic and nicotinic ACh receptors would be activated. Hyperglycemia was prevented and β-cells were preserved because of a shift in the pancreatic T-cell differentiation pattern, from Th17 to Th1, with IFNγ playing a major role (22). Our study complements these prior studies (21, 22) and further demonstrates that T1D development can be mitigated with a short pretreatment and daily administration of a highly specific α7R agonist to impact β-cell STAT3-driven anti-inflammatory and prosurvival signaling. Although it is likely that PNU-282987 treatment in the context of MLDS leads to a similar anti-inflammatory shift in pancreatic T-cell polarization, additional work is needed to determine whether this is indeed the case.

Pharmacologic manipulation of α7R signaling may have therapeutic potential for treating autoimmune diabetes. Although PNU-282987 is not suitable for human use because of off-target effects (43), this class of drugs is being tested for treating schizophrenia and neurodegenerative disorders. Future studies are warranted to explore similar compounds with potent α7R agonist activity that can be tested for reducing inflammatory drive and improving β-cell survival and function in T1D.

In summary, we have demonstrated that systemic α7nAChR activation in mice progressively improves STZ-induced hyperglycemia and β-cell failure by retaining functional BCM, and the mechanism underlying BCM restoration is, in part, because of β-cell α7R activation eliciting both STAT3-dependent anti-inflammatory drive and CREB/Irs2/Akt/Pdx1 prosurvival signaling pathways. Thus, β-cell α7Rs function to maintain β-cell survival and mass homeostasis through modulating islet cytokine and Akt-dependent signaling.

Experimental procedures

Reagents for α7nAChR manipulation

The partial agonist GTS-21 (Tocris Bioscience) and the specific agonist PNU-282987 (Alomone Labs) were used for α7R activation, whereas MLA (Tocris) was used as a specific α7R

antagonist. Tissue culture reagents (media, FCS, and antibiotics) were purchased from Gibco/Thermo Fisher Scientific, and general chemicals and reagents were purchased from Sigma.

Studies using the INS-1 β-cells

Proinflammatory cytokine challenge (TNFα, IL-1β, and IFNγ) of INS-1 cells in the presence of α7R agonist and antagonist—INS-1 (832/13) cells were maintained in RPMI 1640 containing 10% fetal bovine serum, 8.3 mmol/liter glucose, 10 mmol/liter HEPES, 100 mmol/liter L-glutamine, 50 mmol/liter sodium pyruvate, 100 units/ml penicillin, 100 μg/ml streptomycin, and 50 μmol/liter β-mercaptoethanol. The experimental INS-1 cells were pretreated (1 h) with vehicle (DMSO), α7R agonist PNU-282987 (100 μM), or α7R antagonist MLA (100 nM) in the experimental media followed by a 5-h incubation in heat-inactivated serum–supplemented media with a 1× cytokine mixture (human TNFα, IL-1β, and IFNγ: 1000× mixture containing 5 μg/ml IL-1, 10 μg/ml TNFα, and 100 μg/ml IFNγ (ProSpec Technologies)) with the continued presence of PNU and MLA. The cells were washed with PBS and lysed using lysis buffer (50 mmol/liter HEPES, 150 mmol/liter NaCl, 1% Triton X-100, 5 mmol/liter EDTA, 5 mmol/liter EGTA, 20 mmol/liter sodium pyrophosphate, 20 mmol/liter sodium fluoride, 1 mmol/liter activated sodium orthovanadate, 1 mmol/liter phenylmethylsulfonyl fluoride, and 1× protease inhibitors mixture containing 1 μg/ml each leupeptin, aprotinin, and pepstatin A).

Immunoblotting—INS-1 cell lysate proteins (25 μg) were separated by SDS-PAGE and electrophoretically transferred onto polyvinylidene difluoride membranes (Bio-Rad Laboratories). Membranes were incubated overnight at 4 °C with one of the following antibodies: total STAT3 (rabbit monoclonal, Cell Signaling Technology), phospho-STAT3–Tyr^{705} (rabbit monoclonal, Cell Signaling), phospho-NF-κB–Ser^{536} (rabbit monoclonal, Cell Signaling), iNOS/NOS2 (rabbit polyclonal, Millipore), IRS-2 (rabbit polyclonal, Cell Signaling Technology), phospho-Akt–Ser^{473} (rabbit monoclonal, Cell Signaling Technology), total Akt1 (rabbit monoclonal, Cell Signaling Technology), total CREB (rabbit polyclonal, Cell Signaling Technology), phospho-CREB–Ser^{133}, and Pdx1 (rabbit polyclonal, Millipore). Immunoblot membranes were washed and incubated with goat anti-rabbit horseradish peroxidase–conjugated antibody (Bio-Rad) 1 h at room temperature. Detection was by chemiluminescence (Western Thunder, Thermo Fisher Scientific), and autoradiography was performed using HyperFilm-ECL (GE Amersham Biosciences). Immunoblots were stripped and reprobed to establish equivalent loading using anti-β-actin (rabbit polyclonal, Cell Signaling Technology).

Establishing stable knockdown of STAT3 in INS-1 cells—Four 29mer shRNA plasmids in a retroviral GFP vector (pGFP-V-RS) directed against rat STAT3 (Origene, GI737473: 5′-GTCCTCTATCAGCACAACCTGCGAAGAAT-3′; GI737474: 5′-CAGAGCAGGTATCTTGAGAAGCCAATGGA-3′; GI737475: 5′-ACTGGATAACTTCATTAGCAGAATCTCAA-3′; and GI737476: 5′-TTCTTCACTAAGCCTCCGATTGGAACCTG-3′) along with a scrambled control sequence (5′-GCACTACCAGAGCTAACTCAGATAGTACT-3′) were propagated in *Escherichia coli*, and plasmid DNA was isolated

using a midi-prep kit (Qiagen). INS-1 cells (60% confluency, 10-cm plates) were transfected with either a single shRNA or pooling of four shRNA (20 μg of plasmid DNA along with a scrambled control using Lipofectamine 2000 (Invitrogen)). At 24 h post-transfection, the INS-1 cells underwent puromycin selection (1.0 μg/ml) for 3 weeks. The puromycin-resistant/GFP-positive clones expressed STAT3 shRNA or scrambled shRNA. We screened ~30 clones for stable KD of STAT3 by Western blot screening and used a clone yielding a maximum 60% reduction of STAT3 protein levels compared with the scrambled control. These stable clones of INS-1 cells, maintained under puromycin selection (0.5 μg/ml), were used for the cytokine challenge (TNFα, IL-1β, and IFNγ) in the presence and absence of the α7R agonist PNU-282987 as described above. The cell lysates (25 μg of protein) were processed and immunoblotted for the measuring of iNOS, phospho-NF-κB, and total and phospho-STAT3 levels.

Isolated islet studies

Mouse islets were isolated from 10–12-week-old male C57BL/6NTac mice (B6N, Taconic) and *Chrna7* null mice (detailed below) by pancreatic duct infiltration with collagenase, Histopaque gradient separation, and hand picking. The basal mRNA expression of α7R in the mouse islets was detected by RT-PCR using verified *Chrna7* primers (forward, 5′-TTGCCAGTATCTCCCTCCAG-3′; and reverse, 5′-CTTCTCATTCCTTTTGCCAG-3′). The thermal cycle program used an initial denaturing step at 94 °C for 5 min followed by 25 cycles (94 °C for 15 s, 51 °C for 30 s, and 72 °C for 1 min) and a final extension step of 10 min at 72 °C. The isolated mouse islet lysates were used to detect α7R protein expression using a rabbit polyclonal antibody (Sigma-Aldrich). The proinflammatory cytokine (TNFα, IL-1β, and IFNγ) challenge experiments were performed in overnight cultured mouse islets (WT, Het, and KO of *Chrna7*) under experimental conditions similar to those used for INS-1 cells (described above). The islet lysates (20 μg) were used for the Western blot analysis of iNOS, phospho-NF-κB, total and phospho-STAT3 levels, IRS-2, total and phospho-Akt, Pdx1, and total and phospho-CREB. Immunoblots were stripped and reprobed to establish equivalent loading using anti-β-actin (rabbit polyclonal, Cell Signaling Technology).

Animal studies

Ten- to 12-week-old male B6N WT mice (Taconic) and α7nAChR (*Chrna7*) null mice in the B6 background (The Jackson Laboratory (JAX), B6.129S7-*Chrna7*tm1Bay/J)) were utilized in comparative, interventional, and cultured islet studies. *Chrna7* null mice were obtained by crossing heterozygous mice, and PCR genotyping was done as detailed by JAX. All mice were acclimatized to the University of Vermont Animal Facility for 1 week before use. Mice were maintained *ad libitum* on a standard chow diet and a 12/12-h light/dark cycle. Male mice were chosen for diabetes induction studies because female B6 mice are relatively refractory to experimentally induced diabetes (44). For interventional studies, either GTS-21 or PNU-282987 (10 mg/kg) or vehicle (DMSO/sterile PBS, 5:8) was administered i.p. daily starting

at day 7. STZ (Sigma) was prepared freshly daily in 10 mmol/liter citrate buffer, pH 4.0. T1D was induced using a standard MLDS method using 50 mg/kg/day for 5 days starting at day 10. After obtaining University of Vermont Institutional Animal Use and Care Committee approval, the guidelines were strictly followed for these studies.

Glucose homeostasis measurements

Starting at day 15, daily fed-blood glucose concentration (FreeStyle monitor, Abbott) was measured on B6N mice. At 4 days and at 2 and 4 weeks following a 6-h fast, an IPGTT (2 g/kg) was performed ($n = 5$/group) by sampling glucose concentrations at 0, 15, 30, 60, 90, and 120 min. Plasma insulin concentration was measured at 0, 15, 30, and 120 min using a mouse ELISA kit (ALPCO).

Pancreas morphometry and immunofluorescence

After 2 and 4 weeks, B6N mice were euthanized by exsanguination following i.p. sodium pentobarbital ($n = 5$/group). Pancreata were rapidly procured, fixed in 4.0% paraformaldehyde, and routinely processed for paraffin embedding, and a planimetric method was used to measure BCM as detailed previously (30, 45). The relative size distribution of islets and small endocrine cell clusters was measured using established methods (30, 45). We have used relative size distribution previously to provide insight into potential new islet growth or neogenesis. β-Cell proliferation frequency was measured using the nuclear marker Ki-67 as detailed previously (30). Individual β-cell size was measured using the membrane marker pan-cadherin as detailed (30, 45). For determination of apoptotic β-cells, a modified TUNEL staining protocol using a DeadEnd TUNEL labeling kit (Promega) was used followed by streptavidin-Alexa Fluor 647 (Invitrogen) with anti-insulin and 4′,6-diamidino-2-phenylindole (DAPI) nuclear counterstaining, measuring 5 mice/group. Morphometric data were acquired and analyzed using a Nikon Ti-E workstation and NIS Elements software. For each morphometric assay, 5 mice/group were included. For semiquantitative immunofluorescence studies of key β-cell transcription and survival factors, sections were batch co-immunolabeled for insulin and Pdx1 (Developmental Studies Hybridoma Bank, University of Iowa), MafA (Bethyl Laboratories), or phospho-CREB (Cell Signaling Technology), imaged using a $60\times$ oil PlanApo objective with identical settings, and analyzed as detailed previously (27, 30).

Statistical analyses

Data are presented as mean $\pm$ S.E. as indicated. Statistical significance ($p < 0.05$) was determined by one-way analysis of variance or the unpaired Student's *t* test, as indicated, and plotted using GraphPad Prism 7.0.

References

1. Bending, D., Zaccone, P., and Cooke, A. (2012) Inflammation and type one diabetes. *Int. Immunol.* **24,** 339–346 CrossRef Medline
2. Mathis, D., Vence, L., and Benoist, C. (2001) β-Cell death during progression to diabetes. *Nature* **414,** 792–798 CrossRef Medline
3. Mellado-Gil, J., Rosa, T. C., Demirci, C., Gonzalez-Pertusa, J. A., Velazquez-Garcia, S., Ernst, S., Valle, S., Vasavada, R. C., Stewart, A. F., Alonso, L. C., and Garcia-Ocaña, A. (2011) Disruption of hepatocyte growth factor/c-Met signaling enhances pancreatic β-cell death and accelerates the onset of diabetes. *Diabetes* **60,** 525–536 CrossRef Medline
4. Woods, S. C., and Porte, D. Jr. (1974) Neural control of the endocrine pancreas. *Physiol. Rev.* **54,** 596–619 CrossRef Medline
5. Czura, C. J., and Tracey, K. J. (2005) Autonomic neural regulation of immunity. *J. Intern. Med.* **257,** 156–166 CrossRef Medline
6. Pavlov, V. A., and Tracey, K. J. (2012) The vagus nerve and the inflammatory reflex-linking immunity and metabolism. *Nat. Rev. Endocrinol.* **8,** 743–754 CrossRef Medline
7. Rosas-Ballina, M., and Tracey, K. J. (2009) The neurology of the immune system: neural reflexes regulate immunity. *Neuron* **64,** 28–32 CrossRef Medline
8. Drago, J., McColl, C. D., Horne, M. K., Finkelstein, D. I., and Ross, S. A. (2003) Neuronal nicotinic receptors: Insights gained from gene knockout and knockin mutant mice. *Cell. Mol. Life Sci.* **60,** 1267–1280 CrossRef Medline
9. Downs, A. M., Bond, C. E., and Hoover, D. B. (2014) Localization of α7 nicotinic acetylcholine receptor mRNA and protein within the cholinergic anti-inflammatory pathway. *Neuroscience* **266,** 178–185 CrossRef Medline
10. Rosas-Ballina, M., Ochani, M., Parrish, W. R., Ochani, K., Harris, Y. T., Huston, J. M., Chavan, S., and Tracey, K. J. (2008) Splenic nerve is required for cholinergic antiinflammatory pathway control of TNF in endotoxemia. *Proc. Natl. Acad. Sci. U.S.A.* **105,** 11008–11013 CrossRef Medline
11. Delbro, D. S. (2012) Expression of the non-neuronal cholinergic system in rat β-cells. *Auton. Neurosci.* **167,** 75–77 CrossRef Medline
12. Yoshikawa, H., Hellström-Lindahl, E., and Grill, V. (2005) Evidence for functional nicotinic receptors on pancreatic beta cells. *Metabolism* **54,** 247–254 CrossRef Medline
13. Rodriguez-Diaz, R., Dando, R., Jacques-Silva, M. C., Fachado, A., Molina, J., Abdulreda, M. H., Ricordi, C., Roper, S. D., Berggren, P. O., and Caicedo, A. (2011) Alpha cells secrete acetylcholine as a non-neuronal paracrine signal priming beta cell function in humans. *Nat. Med.* **17,** 888–892 CrossRef Medline
14. Ganic, E., Singh, T., Luan, C., Fadista, J., Johansson, J. K., Cyphert, H. A., Bennet, H., Storm, P., Prost, G., Ahlenius, H., Renström, E., Stein, R., Groop, L., Fex, M., and Artner, I. (2016) MafA-controlled nicotinic receptor expression is essential for insulin secretion and is impaired in patients with type 2 diabetes. *Cell Rep.* **14,** 1991–2002 CrossRef Medline
15. Eizirik, D. L., and Mandrup-Poulsen, T. (2001) A choice of death: The signal-transduction of immune-mediated beta-cell apoptosis. *Diabetologia* **44,** 2115–2133 CrossRef Medline
16. Darnell, J. E., Jr., Kerr, I. M., and Stark, G. R. (1994) Jak-STAT pathways and transcriptional activation in response to IFNs and other extracellular signaling proteins. *Science* **264,** 1415–1421 CrossRef Medline
17. Andersson, A. K., Börjesson, A., Sandgren, J., and Sandler, S. (2005) Cytokines affect PDX-1 expression, insulin and proinsulin secretion from iNOS deficient murine islets. *Mol. Cell. Endocrinol.* **240,** 50–57 CrossRef Medline
18. Koster, J. C., Marshall, B. A., Ensor, N., Corbett, J. A., and Nichols, C. G. (2000) Targeted overactivity of beta cell K(ATP) channels induces profound neonatal diabetes. *Cell* **100,** 645–654 CrossRef Medline
19. Zumsteg, U., Frigerio, S., and Holländer, G. A. (2000) Nitric oxide production and Fas surface expression mediate two independent pathways of

cytokine-induced murine beta-cell damage. *Diabetes* **49,** 39 – 47 CrossRef Medline

20. Gautam, D., Han, S. J., Hamdan, F. F., Jeon, J., Li, B., Li, J. H., Cui, Y., Mears, D., Lu, H., Deng, C., Heard, T., and Wess, J. (2006) A critical role for beta cell M3 muscarinic acetylcholine receptors in regulating insulin release and blood glucose homeostasis *in vivo*. *Cell Metab.* **3,** 449 – 461 CrossRef Medline

21. Mabley, J. G., Pacher, P., Southan, G. J., Salzman, A. L., and Szabó, C. (2002) Nicotine reduces the incidence of type I diabetes in mice. *J. Pharmacol. Exp. Ther.* **300,** 876 – 881 CrossRef Medline

22. George, J. A., Bashir, G., Qureshi, M. M., Mohamed, Y. A., Azzi, J., Al-Ramadi, B. K., and Fernández-Cabezudo, M. J. (2016) Cholinergic stimulation prevents the development of autoimmune diabetes: Evidence for the modulation of Th17 effector cells via an IFNγ-dependent mechanism. *Front. Immunol.* **7,** 419 Medline

23. Ali, M. A., El-Abhar, H. S., Kamel, M. A., and Attia, A. S. (2015) Antidiabetic effect of galantamine: Novel effect for a known centrally acting drug. *PLoS One* **10,** e0134648 CrossRef Medline

24. de Jonge, W. J., van der Zanden, E. P., The, F. O., Bijlsma, M. F., van Westerloo, D. J., Bennink, R. J., Berthoud, H. R., Uematsu, S., Akira, S., van den Wijngaard, R. M., and Boeckxstaens, G. E. (2005) Stimulation of the vagus nerve attenuates macrophage activation by activating the Jak2-STAT3 signaling pathway. *Nat. Immunol.* **6,** 844 – 851 CrossRef Medline

25. Yu, Z., Zhang, W., and Kone, B. C. (2002) Signal transducers and activators of transcription 3 (STAT3) inhibits transcription of the inducible nitric oxide synthase gene by interacting with nuclear factor κB. *Biochem. J.* **367,** 97 – 105 CrossRef Medline

26. Yu, Z., and Kone, B. C. (2004) The STAT3 DNA-binding domain mediates interaction with NF-κB p65 and inducible nitric oxide synthase transrepression in mesangial cells. *J. Am. Soc. Nephrol.* **15,** 585 – 591 CrossRef Medline

27. Lausier, J., Diaz, W. C., Roskens, V., LaRock, K., Herzer, K., Fong, C. G., Latour, M. G., Peshavaria, M., and Jetton, T. L. (2010) Vagal control of pancreatic β-cell proliferation. *Am. J. Physiol. Endocrinol. Metab.* **299,** E786 – E793 CrossRef Medline

28. Maier, B., Ogihara, T., Trace, A. P., Tersey, S. A., Robbins, R. D., Chakrabarti, S. K., Nunemaker, C. S., Stull, N. D., Taylor, C. A., Thompson, J. E., Dondero, R. S., Lewis, E. C., Dinarello, C. A., Nadler, J. L., and Mirmira, R. G. (2010) The unique hypusine modification of eIF5A promotes islet beta cell inflammation and dysfunction in mice. *J. Clin. Invest.* **120,** 2156 – 2170 CrossRef Medline

29. Kitagawa, H., Takenouchi, T., Azuma, R., Wesnes, K. A., Kramer, W. G., Clody, D. E., and Burnett, A. L. (2003) Safety, pharmacokinetics, and effects on cognitive function of multiple doses of GTS-21 in healthy, male volunteers. *Neuropsychopharmacology* **28,** 542 – 551 CrossRef Medline

30. Jetton, T. L., Lausier, J., LaRock, K., Trotman, W. E., Larmie, B., Habibovic, A., Peshavaria, M., and Leahy, J. L. (2005) Mechanisms of compensatory beta-cell growth in insulin-resistant rats: Roles of Akt kinase. *Diabetes* **54,** 2294 – 2304 CrossRef Medline

31. Vinik, A. I. (2012) The conductor of the autonomic orchestra. *Front. Endocrinol.* (*Lausanne*) **3,** 71 Medline

32. Mundinger, T. O., and Taborsky, G. J. (2016) Early sympathetic islet neuropathy in autoimmune diabetes: Lessons learned and opportunities for investigation. *Diabetologia* **59,** 2058 – 2067 CrossRef Medline

33. Saravia, F., and Homo-Delarche, F. (2003) Is innervation an early target in autoimmune diabetes? *Trends Immunol.* **24,** 574 – 579 CrossRef Medline

34. Zhang, B., Yang, L., Yu, L., Lin, B., Hou, Y., Wu, J., Huang, Q., Han, Y., Guo, L., Ouyang, Q., Zhang, B., Lu, L., and Zhang, X. (2012) Acetylcholinesterase is associated with apoptosis in β cells and contributes to insulin-dependent diabetes mellitus pathogenesis. *Acta Biochim. Biophys. Sin.* (*Shanghai*) **44,** 207 – 216 CrossRef Medline

35. Koopman, F. A., Vosters, J. L., Roescher, N., Broekstra, N., Tak, P. P., and Vervoordeldonk, M. J. (2015) Cholinergic anti-inflammatory pathway in the non-obese diabetic mouse model. *Oral Dis.* **21,** 858 – 865 CrossRef Medline

36. Kiba, T. (2002) The role of the autonomic nervous system in liver regeneration and apoptosis-recent developments. *Digestion* **66,** 79 – 88 CrossRef Medline

37. Edvell, A., and Lindström, P. (1998) Vagotomy in young obese hyperglycemic mice: Effects on syndrome development and islet proliferation. *Am. J. Physiol. Endocrinol. Metab.* **274,** E1034 – E1039 Medline

38. Imai, J., Katagiri, H., Yamada, T., Ishigaki, Y., Suzuki, T., Kudo, H., Uno, K., Hasegawa, Y., Gao, J., Kaneko, K., Ishihara, H., Niijima, A., Nakazato, M., Asano, T., Minokoshi, Y., and Oka, Y. (2008) Regulation of pancreatic beta cell mass by neuronal signals from the liver. *Science* **322,** 1250 – 1254 CrossRef Medline

39. Yamamoto, J., Imai, J., Izumi, T., Takahashi, H., Kawana, Y., Takahashi, K., Kodama, S., Kaneko, K., Gao, J., Uno, K., Sawada, S., Asano, T., Kalinichenko, V. V., Susaki, E. A., Kanzaki, M., *et al.* (2017) Neuronal signals regulate obesity induced β-cell proliferation by FoxM1 dependent mechanism. *Nat. Commun.* **8,** 1930 Medline

40. Fujimoto, K., and Polonsky, K. S. (2009) Pdx1 and other factors that regulate pancreatic beta-cell survival. *Diabetes Obes. Metab.* **11,** Suppl. 4, 30 – 37 Medline

41. Klee, P., Bosco, D., Guérardel, A., Somm, E., Toulotte, A., Maechler, P., and Schwitzgebel, V. M. (2016) Activation of nicotinic acetylcholine receptors decreases apoptosis in human and female murine pancreatic islets. *Endocrinology* **157,** 3800 – 3808 CrossRef Medline

42. Xu, T. Y., Guo, L. L., Wang, P., Song, J., Le, Y. Y., Viollet, B., and Miao, C. Y. (2012) Chronic exposure to nicotine enhances insulin sensitivity through α7 nicotinic acetylcholine receptor-STAT3 pathway. *PLoS One* **7,** e51217 CrossRef Medline

43. Walker, D. P., Wishka, D. G., Piotrowski, D. W., Jia, S., Reitz, S. C., Yates, K. M., Myers, J. K., Vetman, T. N., Margolis, B. J., Jacobsen, E. J., Acker, B. A., Groppi, V. E., Wolfe, M. L., Thornburgh, B. A., Tinholt, P. M., Cortes-Burgos, L. A., *et al.* (2006) Design, synthesis, structure-activity relationship, and *in vivo* activity of azabicyclic aryl amides as α7 nicotinic acetylcholine receptor agonists. *Bioorg. Med Chem.* **14,** 8219 – 8248 CrossRefMedline

44. Kolb, H. (1987) Mouse models of insulin dependent diabetes: Low-dose streptozocin-induced diabetes and nonobese diabetic (NOD) mice. *Diabetes Metab. Rev.* **3,** 751 – 778 CrossRef Medline

45. Jetton, T. L., Everill, B., Lausier, J., Roskens, V., Habibovic, A., LaRock, K., Gokin, A., Peshavaria, M., and Leahy, J. L. (2008) Enhanced beta-cell mass without increased proliferation following chronic mild glucose infusion. *Am. J. Physiol. Endocrinol. Metab.* **294,** E679 – E687 CrossRef Medline

ASBMB